Journal of Molecular Catalysis A: Chemical 353–354 (2012) 67–73

Contents lists available at SciVerse ScienceDirect

Journal of Molecular Catalysis A: Chemical

journal homepage: www.elsevier.com/locate/molcata

Room-temperature synthesis and photocatalytic properties of lepidocrocite by monowavelength visible light irradiation

Yulong Lin[a,b,d], Yu Wei[c,*], Yuhan Sun[a,**]

[a] Institute of Coal Chemistry, Chinese Academy of Science, Taiyuan 030001, China
[b] Graduate School of the Chinese Academy of Sciences, Beijing 100039, China
[c] College of Chemistry and Materials Science, Hebei Normal University, Shijiazhuang 050016, China
[d] School of Pharmaceutical Sciences, Hebei Medical University, Shijiazhuang 050017, China

ARTICLE INFO

Article history:
Received 3 August 2011
Received in revised form 10 October 2011
Accepted 1 November 2011
Available online 7 November 2011

Keywords:
Lepidocrocite
Photocatalytic oxidation
Decolorization
Crystal violet
Monowavelength

ABSTRACT

Lepidocrocite was synthesized by aerial oxidation using an Fe^{II}EDTA solution. The synthesis was performed under irradiation from different monowavelength light emitting diode (LED) lamps at room temperature. X-ray diffraction results showed the formation of differently crystallized lepidocrocite. The indirect bandgap values of the lepidocrocite samples were about 2.34, 2.36, and 2.31 eV for red, green, and blue light, respectively. The kinetics of the photo-decolorization of crystal violet (CV) was investigated in a system composed of lepidocrocite, H_2O_2, and visible light. H_2O_2 concentration, light irradiation, and catalyst concentration were also investigated. The rate of CV decolorization was found to fit pseudo-first-order kinetics. The results show that different as-prepared lepidocrocite have different adsorption and photocatalytic characteristics. A possible mechanism was also suggested for the dye degradation.

1. Introduction

In recent years, lepidocrocite (γ-FeOOH) has been used as a functional material in Fenton-like reactions and photocatalytic processes for environmental applications. Such applications include the photodegradation of chelators and organic dyes, as well as the photolysis of heavy metal salts [1–3]. Therefore, the preparation of highly active lepidocrocite is important in modern materials chemistry. The unique way to form lepidocrocite is the oxidation of $Fe(OH)_2$ by air in suspension at pH around 7 [4]. Previous studies have revealed that both visible light and the presence of ethylenediaminetetraacetic acid (EDTA) could accelerate the reaction rate of lepidocrocite [5,6]. An Fe^{II}EDTA complex forms and exhibits strong ligand-to-metal charge absorption in the near-ultraviolet (UV) and visible regions [7–9]. A rapid reaction is favorable for the formation of γ-FeOOH at pH 8.0. However, high-power visible light sources release large amounts of heat, which lead to increased reaction temperature and wasted energy. If a specific wavelength range in favor of the reaction is found, the only thing necessary to irradiate the reaction is a light source emitting the specific wavelength. Consequently, light and power energies would be economized, which would be conducive to industrial production. To the best of our knowledge, the influence of wavelengths on the synthesis of iron oxide particles in the presence of EDTA has not yet been reported. In the present work, we examine the role of the wavelengths of light emitting diode (LED) visible light on the preparation and performance of γ-FeOOH. The physical and optical properties of lepidocrocite are also investigated.

Crystal violet (CV) is a recalcitrant triphenylmethane dye used in textiles and printing and a recalcitrant molecule [10,11]. The decolorization of wastewaters containing CV is mandated by most countries. Several physicochemical and microbial biodegradation methods have been used to decolorize wastewater effluents [12–14]. A very simple, commonly utilized approach is the photocatalytic oxidation of such dyes. In the present paper, the relative efficiencies of different γ-FeOOH samples for CV dye degradation were examined. H_2O_2 concentration, light irradiation, and catalyst concentration were also investigated. Furthermore, a possible degradation mechanism was also suggested.

2. Experimental

2.1. Chemicals and materials

Sodium hydroxide (NaOH), ethylenediaminetetraacetic acid (EDTA), and sulfuric acid (H_2SO_4) were purchased from Tianjin Yongda Chemical Reagents. Crystal violet (CV), with around 90% dye

* Corresponding author. Tel.: +86 311 86268342; fax: +86 311 86268342.
** Corresponding author.
E-mail addresses: weiyu@mail.hebtu.edu.cn (Y. Wei), yhsun@sxicc.ac.cn (Y. Sun).

1381-1169/$ – see front matter © 2011 Elsevier B.V. All rights reserved.
doi:10.1016/j.molcata.2011.11.006

content, was obtained from Tianjin Hengxing Reagents. All chemicals were of analytical purity and used without further purification. Aqueous ferrous sulfate ($FeSO_4$) solution was prepared by dissolving iron granules in 20% H_2SO_4. Distilled water was used as solvent for the reactions.

2.2. Synthesis of γ-FeOOH

Appropriate amounts of EDTA (0.05 M) and $FeSO_4$ (1.0 M) were mixed in a 250 mL beaker. An NaOH solution (1.0 M) was used to adjust the pH to 8. The volume of the solution was adjusted to 100 mL with distilled water. Air was then passed at a rate of 0.272 m^3/h through the suspension under irradiation with 12 W monowavelength visible light LED lamps (Tianshengda, China) at 25 °C. The major emissions of red, green, and blue light LEDs were at 625 (L-625), 525 (L-525), and 460 nm (L-460), respectively. Light intensity (E) (setting at 3000 lux) was detected by a light meter (TES-1336A, Taiwan). The change in pH during oxidation was monitored using a digital pH meter. The concentration of Fe (II) (solid and liquid) was monitored during oxidation (titration with standard potassium dichromate solution in the presence of a 1 H_2SO_4:1 H_3PO_4 solution) [15]. The precipitate was collected by filtration, and was washed with distilled water as well as $NH_3{\cdot}H_2O$ (1.0 M), then oven-dried at 40–50 °C for 24 h. The yield of the lepidocrocite under this reaction conditions is about 70%.

2.3. Sample characterizations

X-ray diffraction (XRD) patterns were obtained using a Bruker D8 Advance X-ray diffractometer with monochromatic high-intensity Cu Kα radiation (λ = 1.5418 Å) in a 2θ range of 10–80°. Particle morphology was observed using transmission electron microscopy (TEM, Hitachi H–7650). UV–vis diffuse reflectance spectra (UVDRS) were obtained using a UV–vis spectrometer (U-3010, Hitachi) equipped with an integrating sphere assembly. The specific surface area of the iron oxides was determined by multipoint N_2-BET analysis using a Quantachrome (NOVAe) surface area analyzer.

2.4. Adsorption experiments

The adsorption experiments of CV on the lepidocrocite surface were conducted at 25 °C in the dark at neutral pH. A fixed amount of lepidocrocite (0.020 g) was added to 100 mL of an aqueous CV solution with various concentrations, which remained for 24 h in a vibrator. CV concentrations were measured after equilibrium by a spectrophotometer (VIS-7220 Ruili, Beijing) at a wavelength of 580 nm, using a 1 cm quartz cell, and the amount of CV adsorbed on the lepidocrocite was calculated based on the mass balance according to Eq. (1) [16].

2.5. Measurement of photocatalytic activity

The photocatalytic degradation of CV using different lepidocrocite was carried out as follows.

A fixed amount of lepidocrocite (0.020 g) was added to 100 mL of CV solution (20 μM). The dye and oxyhydroxide were stirred for 30 min in the dark to ensure adsorption equilibrium. H_2O_2 was added to the reaction vessel at the beginning of the irradiation by a 100 W incandescent lamp. The solution pH was adjusted to about 7 with diluted solutions of $HClO_4$ and NaOH. At selected time intervals, 5 mL aliquots were collected, filtered, and analyzed by the spectrophotometer. All experimental runs were performed at 25 °C under continuous stirring in the presence of visible light and air.

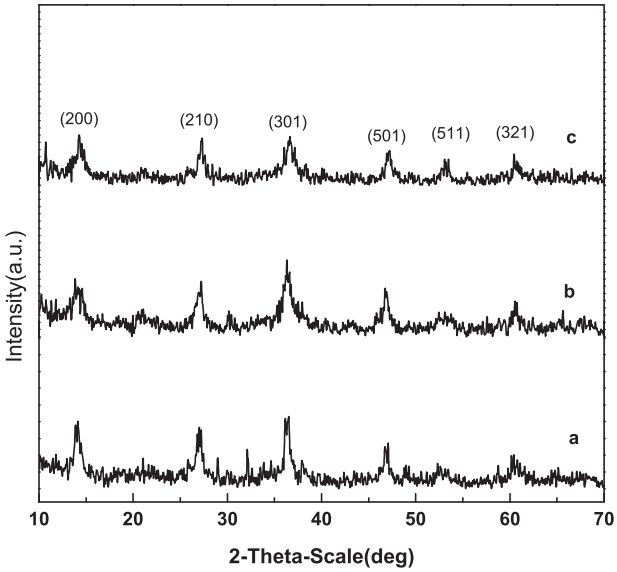

Fig. 1. XRD patterns of the lepidocrocite samples (a) L-625, (b) L-525, and (c) L-460.

Each experiment was performed in triplicates, and all results were expressed as a mean value of the three experiments.

3. Results and discussion

3.1. Characterization of lepidocrocite

The characteristic peaks of the as-prepared samples corresponded very well to the standard card of lepidocrocite (JCPDS: 44-1415) (Fig. 1). The results proved that the samples were γ-FeOOH with a layered structure [4]. FTIR spectra were also examined (shown in supporting information SI 1), the bands at 1021.0 and 746.5 cm^{-1} are assigned to in-plane and out-of-plane Fe–O–H bending vibrations for γ–FeOOH, respectively [4,17]. Sample L-460 (Fig. 1c) irradiated by a blue LED lamp had a weak crystallization, with the widest and weakest peaks. In contrast, L-625 (Fig. 1a) had the highest crystallization.

The TEM and SEM images of the three lepidocrocite samples all displayed flaky shapes (Fig. 2, SI 2). The results showed that the crystallization of L-625 (Fig. 2a) was higher than that of L-525 (Fig. 2b) and L-460 (Fig. 2c). These findings were consistent with those of the XRD (Fig. 1), and were also similar to those in previous works [5].

The difference in reaction rates may be the main reason for the variations observed. In the present system, at the start-up phase, the rate of change in the blue LED lamp system was obviously more rapid than that in the red and green LED lamp system (Fig. 3). During the oxidation of Fe(II), EDTA was chelated with Fe(II), forming Fe^{II}EDTA complexes, which had strong absorption bands in the near-UV and visible regions. Blue light had higher energy than red light, so the oxidation reaction was accelerated in the blue LED lamp system. Crystal seeds of γ-FeOOH formed too rapidly and were too numerous to grow in a short time. Hence, green rust then rapidly transformed into γ-FeOOH with low crystallinity. The relatively lower oxidation speed favored the formation of the high-crystalline phase in the red LED lamp system.

The optical properties of the lepidocrocite samples were studied by UV–vis spectroscopy. The absorption spectra of the three lepidocrocite samples prepared were showed in Fig. 4. Light absorption was high in the short-wavelength region of the spectra. As the wavelength increased, absorption gradually decreased. As the spectra reached the characteristics of the optical absorption

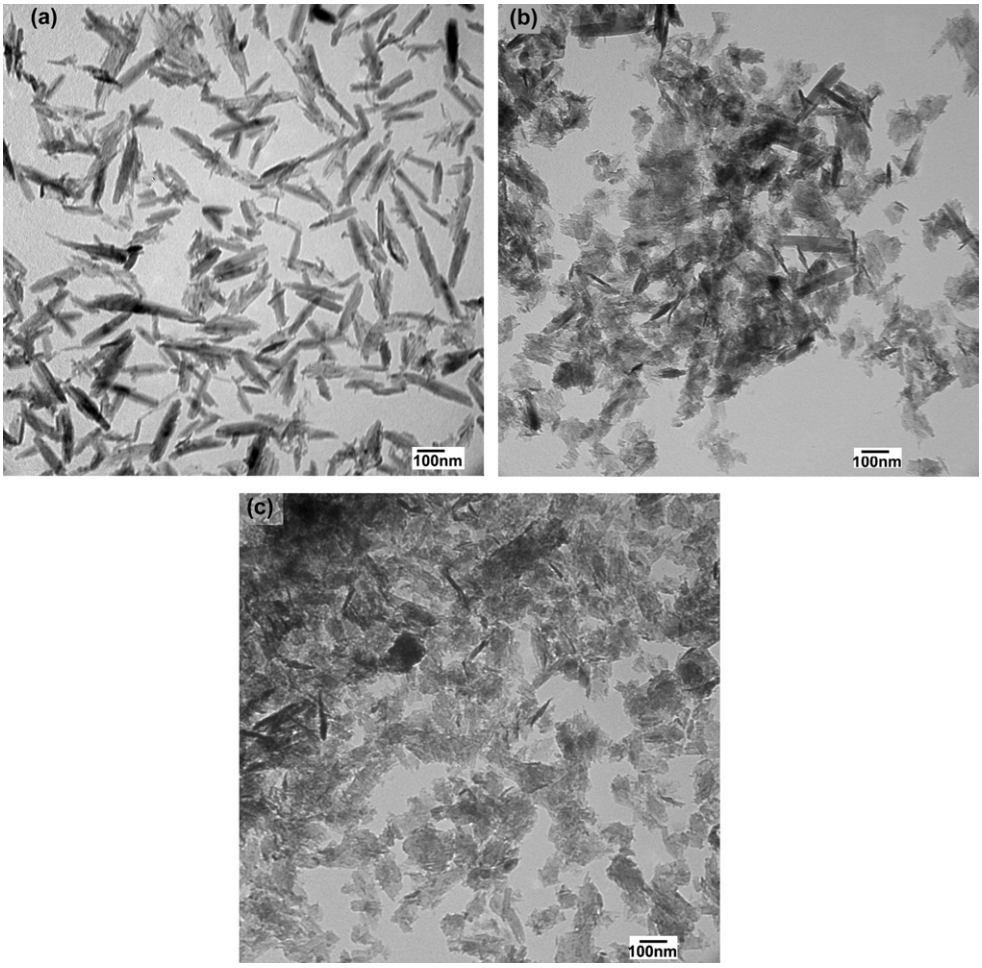

Fig. 2. TEM images of the lepidocrocite samples (a) L-625, (b) L-525, and (c) L-460.

threshold for lepidocrocite (~500 nm), absorption rapidly dropped and extended to the red region as a plateau. The absorption observed after this threshold could be the result of the light-scattering properties of nanoparticles at longer wavelengths. The indirect optical bandgap of lepidocrocite can be estimated by calculating the intercept of the extrapolated linear fit to the experimental data of a plot of $(\alpha hv)^2$ versus incident photon energy (hv) near the absorption edge, where α is the absorption coefficient [18–20]. The inset figure showed $(\alpha hv)^2$ versus photon energy plots for the three lepidocrocite samples. The indirect bandgap values (Eg) measured were 2.34, 2.36, and 2.31 eV for L-625 in red light, L-525

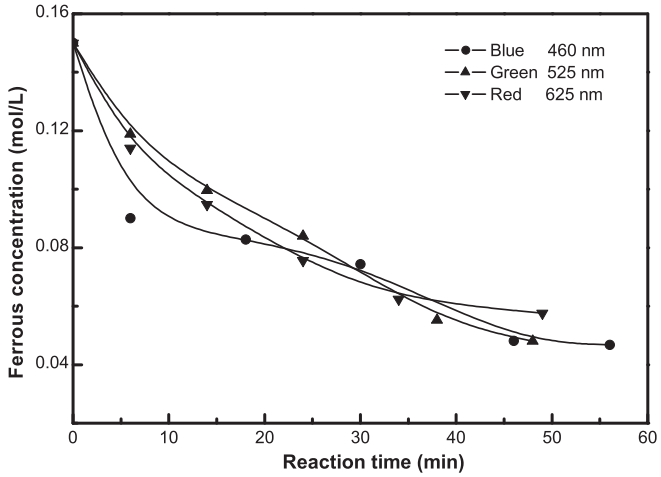

Fig. 3. Changes in Fe(II) concentration with reaction time by different monochromatic LED light at pH 8.

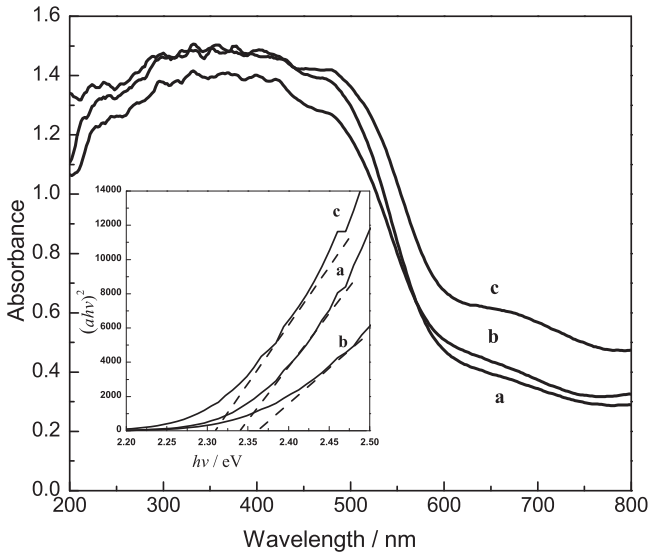

Fig. 4. Absorption spectra of the lepidocrocite samples (a) L-625, (b) L-525, and (c) L-460. The insets show $(\alpha hv)^2$ vs. wavelength plots. The optical bandgap was determined by extrapolation.

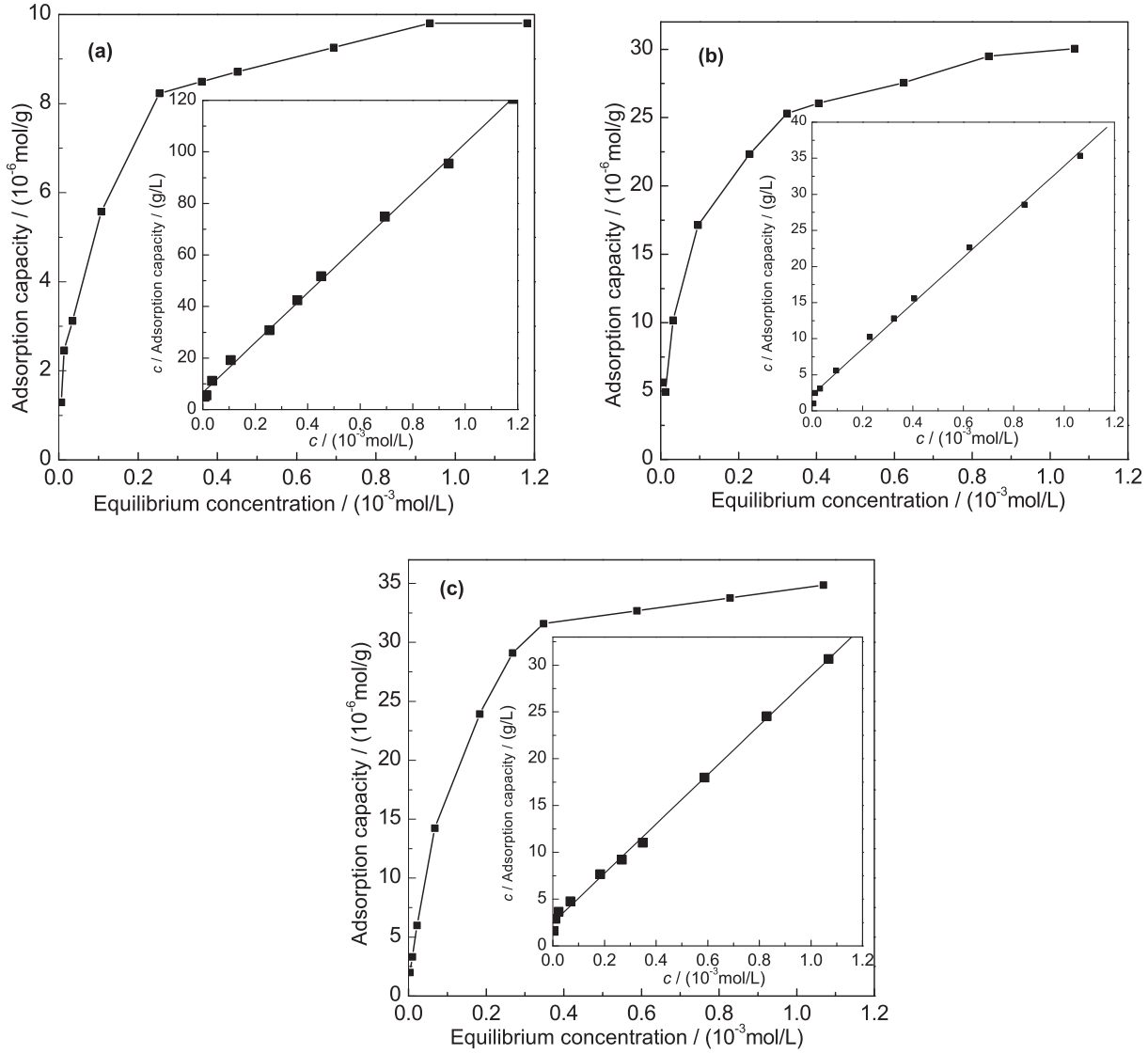

Fig. 5. Adsorption isotherms of crystal violet (20 μM) on the surfaces of the lepidocrocite (0.20 g/L) samples (a) L-625, (b) L-525, and (c) L-460. The insets show Langmuir linear relationship.

in green light, and L-460 in blue light, respectively. These values match that reported in the literature (2.60 eV) [21]. Due to the red shift of spectra, the photocatalytic property of lepidocrocite flakes should have undergone some improvement. A series of photocatalytic experiments were performed with triphenylmethane dyes (CV) used as model pollutant to evaluate photocatalytic activity of γ-FeOOH under visible-light irradiation.

3.2. Adsorption of CV by lepidocrocite

The amount of CV adsorbed by lepidocrocite was calculated based on the mass balance in Eq. (1). The adsorption isotherms of CV for the different lepidocrocite samples are shown in Fig. 5. These isotherms well fitted the Langmuir adsorption model given in Eq. (2) [16,22].

$$\Gamma = \frac{(c_0 - c)V}{m} \quad (1)$$

$$\frac{c}{\Gamma} = \frac{1}{\Gamma_{max}}c + \frac{1}{K_a\Gamma_{max}} \quad (2)$$

Γ and Γ_{max} (mol/g) are the adsorbed concentration and saturated adsorption capacity, respectively. c_0 and c (mol/L) are the initial and equilibrium concentrations of the CV solution, respectively. V (L) is the volume of the solution, and m (g) is the lepidocrocite mass used in each batch. K_a (L/mol) is the adsorption equilibrium constant.

Γ_{max} was ranked in the order of L-460 > L-525K > L-625, whereas K_a was ranked as L-625 > L-525 > L-460 (Table 1). These results implied that both physical and chemical adsorption simultaneously existed between CV and lepidocrocite. A higher physical adsorption corresponded to a large specific surface area and high crystallization. However, a larger K_a denoted a stronger chemical adsorption [2,23].

Table 1
The adsorption parameters of crystal violet by using different lepidocrocite.

Samples	SSA[a] (m^2/g)	Γ_{max}[b] (10^{-5} mol/g)	K_a[c] (10^4 L/mol)	R^2
L-625	41.3	1.03	1.46	0.9982
L-525	53.4	3.15	1.43	0.9969
L-460	60.2	3.79	1.07	0.9974

[a] Specific surface area.
[b] Saturated adsorption capacity.
[c] Adsorption equilibrium constant.

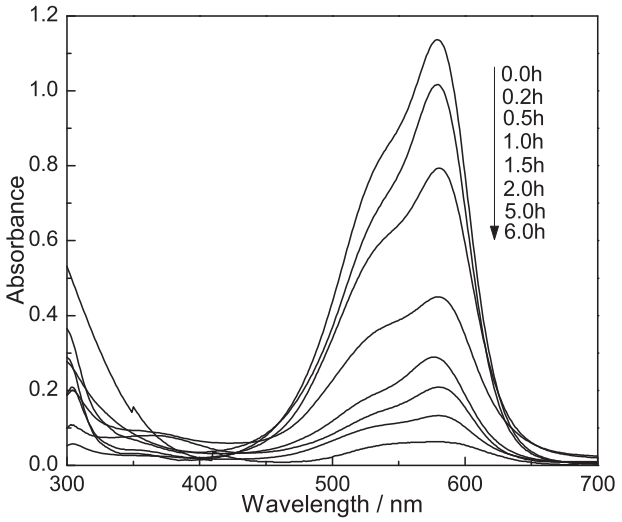

Fig. 6. UV–vis absorption spectral changes of crystal violet in the reaction filtrate with irradiation time. CV: 20 μM, L-460: 200 mg/L, H_2O_2: 2×10^{-3} M, visible light irradiation, and pH 7.

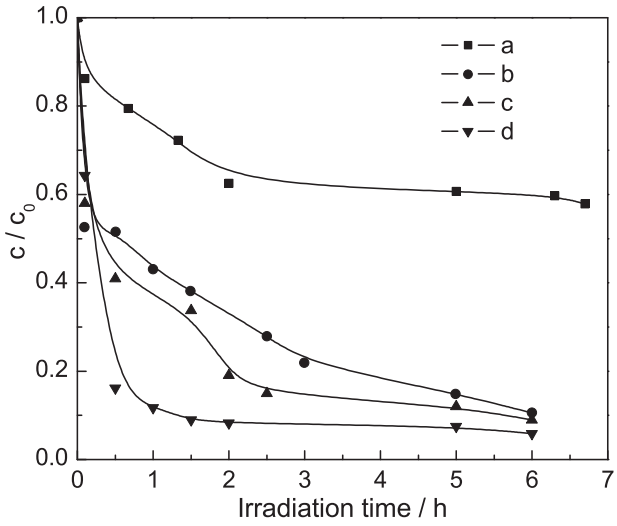

Fig. 8. Effects of catalytic dosage on the decomposition of CV in the aerated suspension of L-460. (a) 0 g/L (b) 0.1 g/L, (c) 0.2 g/L and (d) 0.5 g/L. CV: 20 μM, H_2O_2: 1×10^{-3} M, visible light irradiation, and pH 7.

3.3. Photocatalytic oxidation of CV

The catalytic actions of lepidocrocite obtained by different LED sources on the degradation of CV were investigated. Several parameters that affected the dye decolorization rate, such as H_2O_2 concentration, light irradiation, and dye concentration, were evaluated. The UV–visible spectral changes observed during the degradation of CV in the presence of γ-FeOOH/H_2O_2 systems under visible light illumination are showed in Fig. 6. The maximum absorption at 580 nm decreased with the irradiation time. Concomitantly, the absorption at $\lambda < 400$ nm also increases markedly. The degradation of CV at the end of 6 h irradiation time was about 90%. However, during visible light irradiation, the shifts of characteristic absorption band were not found, which indicated that there might be not formation of N-de-methylated intermediates. Hence, cleavage of the whole conjugated chromophore structure of the CV dye was the dominating process [12,24,25].

Fig. 7 shows the effect of concentration of hydrogen peroxide on the destruction of CV. It is observed that degradation was about 90% on the application of 2×10^{-3} M H_2O_2 (Fig. 7c). It was reduced to 80% at 2×10^{-4} M of H_2O_2 and 0 M of H_2O_2 removed only 40%. Therefore, the optimum concentration of H_2O_2 was considered as 1×10^{-3} M.

Fig. 8 shows a plot of degradation of CV dye versus lepidocrocite concentration. It is important to study the dependence of the photocatalytic reaction rate on the concentration of lepidocrocite in the CV dye. Hence, the effect of photocatalyst concentration was investigated. The dye solution (20 μM) was irradiated for 6 h with different lepidocrocite doses (0, 0.1, 0.2, 0.5 g/L). As expected, the photodegradation rate of CV was found to increase with the increase in lepidocrocite dose. At 0.5 g/L catalytic dose (Fig. 8d), the CV was found to be almost completely decolorized on irradiation for 6 h.

The foregoing results indicated that the combination of lepidocrocite, H_2O_2, and visible light provided the most effective conditions for CV degradation (Fig. 9).

Therefore, this reaction system was used in investigating different lepidocrocite samples (Fig. 10). The L-460 sample provided

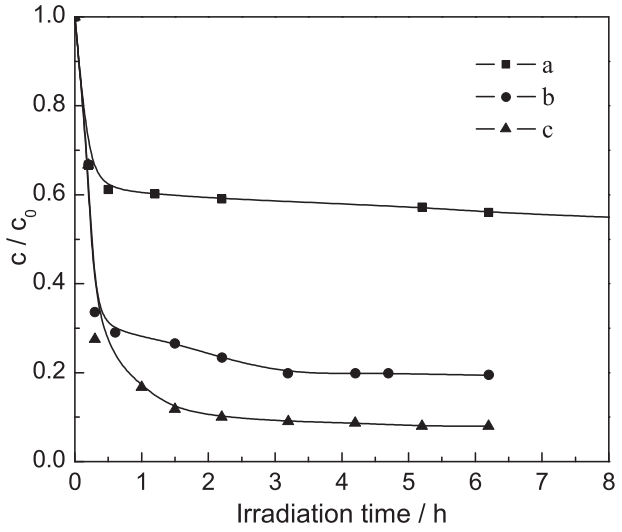

Fig. 7. Concentration effects of H_2O_2 on the photodegradation of CV in the aerated suspension of L-460. (a) 0 M (b) 2×10^{-4} M, and (c) 2×10^{-3} M. CV: 20 μM, L-460: 0.20 g/L, visible light irradiation, and pH 7.

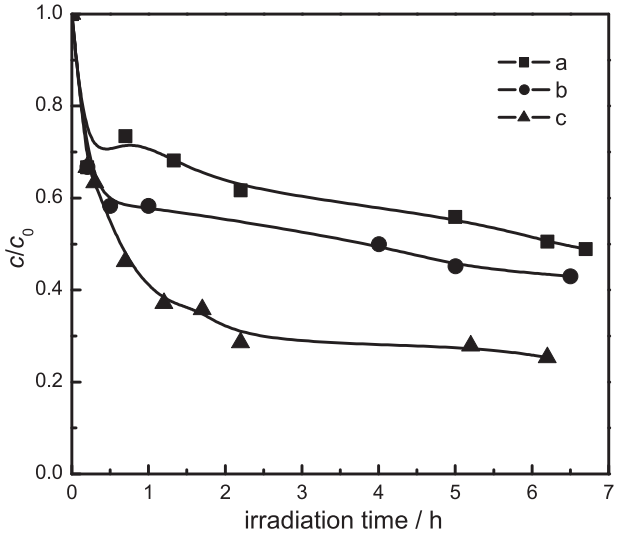

Fig. 9. Kinetics of crystal violet (20 μM) oxidation in the L-460 (0.20 g/L) sample systems. (a) Visible light irradiation, (b) 2.0 mM H_2O_2 in the dark, and (c) 2.0 mM H_2O_2, and visible light irradiation.

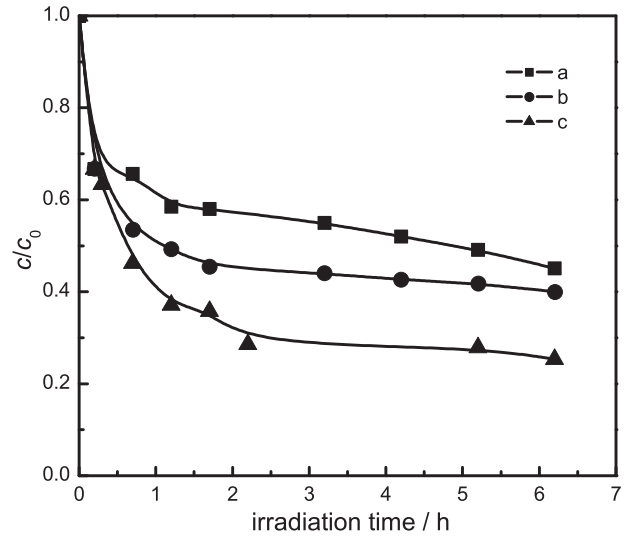

Fig. 10. Photocatalytic oxidation of crystal violet (20 μM) in the presence of different lepidocrocites (0.20 g/L) with 2.0 mM H_2O_2 and visible light irradiation at pH 7. (a) L-625, (b) L-525, and (c) L-460.

the highest decolorization effect (Fig. 10c), whereas L-625 had the lowest effect (Fig. 10a).

The kinetics of CV decolorization in an aqueous solution could be described according to the following pseudo-first-order equation [16,26]:

$$c_t = c_0 \ \exp(-k_a t), \tag{3}$$

where c_0 is the initial CV concentration and k_a is the pseudo-first-order apparent rate constant (h^{-1}). k_a constants were obtained from the slopes of ln (c_0/c_t) versus t plots through regression. The regression results of the experimental data followed the order L-460 (0.40935 h^{-1}) > L-525 (0.06435 h^{-1}) > L-625 (0.05985 h^{-1}). This trend was consistent with the order of the specific surface area and saturated adsorption capacity (Table 1).

3.4. Possible photocatalytic mechanism

To understand the photoreaction process of CV degradation in a lepidocrocite – H_2O_2 system, the interaction of lepidocrocite, H_2O_2, and CV under irradiation was examined.

At near neutral pH values, the solubility of lepidocrocite was smaller. Hence, the degradation of this organic compound followed a heterogeneous Fenton-like reaction. Under this reaction, the electrostatic interactions between the catalyst surface and the organic compound became important [27]. These interactions involved the positively charged CV and the negatively charged lepidocrocite surface, as shown in the following equations [28–32].

$$\equiv\text{Fe(III)–OH} \rightarrow \equiv\text{Fe(III)–O}^- + \text{H}^+ \tag{4}$$

$$\equiv\text{Fe(III)–O}^- + \text{CV}^+ \rightarrow \equiv\text{Fe(III)–O–CV} \tag{5}$$

Given the lower indirect bandgap values, an electron–hole pair was produced when the lepidocrocite catalyst was exposed to visible light, as shown in Eq. (6).

$$\equiv\text{Fe(III)–OH} + h\nu \rightarrow \ e_{cb}{}^- + h_{vb}{}^+ \tag{6}$$

Additional amounts of HO• radicals were also produced from the direct photolysis of H_2O_2 as the Eq. (7).

$$H_2O_2 + h\nu \rightarrow \ HO^\bullet \tag{7}$$

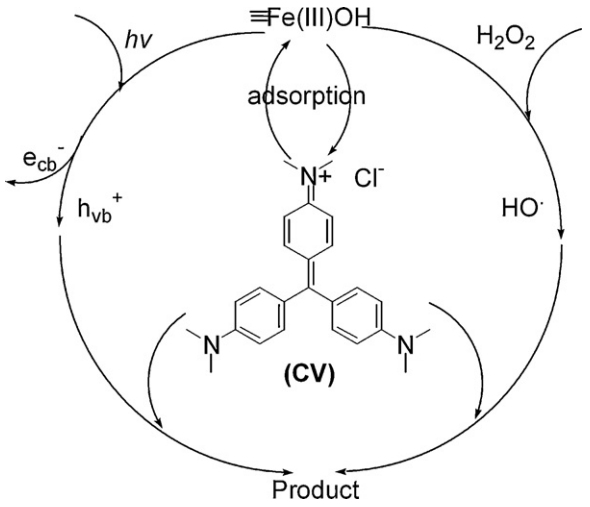

Scheme 1. Schematic for the degradation mechanism of crystal violet by as-prepared γ-FeOOH.

According to the classical Haber–Weiss mechanism, the interactions between the oxidant and iron surfaces are explained in Eqs. (8) and (9).

$$\equiv\text{Fe(III)–OH} + H_2O_2 \rightarrow \equiv\text{Fe(II)–OH} + HO_2^\bullet \tag{8}$$

$$\equiv\text{Fe(II)–OH} + H_2O_2 \rightarrow \equiv\text{Fe(III)–OH} + HO^\bullet + HO^- \tag{9}$$

HO• and $h_{vb}{}^+$ then reacted with the dye to form other species, and were thus responsible for the dye decolorization. Consequently, the surface-adsorbed organic compounds were readily accessible to oxidation by HO• radicals.

$$\equiv\text{Fe(III)–O–CV} + \text{HO}\bullet/h_{vb}{}^+ \rightarrow \rightarrow \ \text{Products} \tag{10}$$

$$\text{CV}* + \text{HO}\bullet/h_{vb}{}^+ \rightarrow \rightarrow \ \text{Products} \tag{11}$$

On the base of the above discussion, possible pathway for the photocatalytic degradation of dyes with γ–FeOOH photocatalyst is shown in Scheme 1.

4. Conclusion

Lepidocrocite samples were synthesized by aerial oxidation using a ferrous solution under different LED visible light irradiation in the presence of trace EDTA at pH 8.0. Different crystallizations were obtained by different oxidation rates. Hence, the saturated adsorption capacities (Γ_{max}) were 3.79×10^{-5}, 3.15×10^{-5}, and 1.03×10^{-5} mol/g for L-460, L-525, and L-625, respectively. The lepidocrocite samples had lower bandgap values, which were 2.34, 2.36, and 2.31 eV for L-625, L-525, and L-460, respectively. The results of the catalytic experiments illustrated the efficiency of lepidocrocite in CV decolorization with traces of H_2O_2 and visible light radiation. Based on these results, a mechanism was proposed. Large amounts of hydroxyl radicals (HO•) were suggested to be simultaneously produced by photo-Fenton and photocatalytic processes.

Acknowledgments

The authors are grateful for the financial support by the National Natural Science Foundation of China under grant nos. 20877021 and 21077031, and the Province Natural Science Foundation of Hebei under grant nos. 08B011 and E2000700274.

Appendix A. Supplementary data

Supplementary data associated with this article can be found, in the online version, at doi:10.1016/j.molcata.2011.11.006.

References

[1] G. Karametaxas, S.J. Hug, B. Sulzberger, Environ. Sci. Technol. 29 (1995) 2992–3000.
[2] J. Lei, C.S. Liu, F.B. Li, X.M. Li, S.G. Zhou, T.X. Liu, M.H. Gu, Q.T. Wu, J. Hazard. Mater. 137 (2006) 1016–1024.
[3] P. Borer, S.J. Hug, B. Sulzberger, S.M. Kraemer, R. Kretzschmar, J. Phys. Chem. C 111 (2007) 10560–10569.
[4] R.M. Cornell, U. Schwertmann, The Iron Oxides, second ed., VCH, New York, 2003.
[5] R.F. Chen, H.X. Chen, Y. Wei, D.L. Hou, J. Phys. Chem. C 111 (2007) 16453–16459.
[6] R.F. Chen, G.Q. Song, Y. Wei, J. Phys. Chem. C 114 (2010) 13409–13413.
[7] Y. Zhou, Y. Deng, Chemosphere 35 (1997) 2051–2058.
[8] Y. Zhou, J. Hoigne, Environ. Sci. Technol. 26 (1992) 1014–1022.
[9] B.C. Faust, R.G. Zepp, Environ. Sci. Technol. 27 (1993) 2517–2522.
[10] W. Azmi, R.K. Sani, U.C. Banerjee, Enzyme Microb. Technol. 22 (1998) 185–191.
[11] S.J. Culp, F.A. Beland, J. Am. Coll. Toxicol 15 (1996) 219–238.
[12] F.A. Alshamsi, A.S. Albadwawi, M.M. Alnuaimi, M.A. Rauf, S.S. Ashraf, Dyes Pigments 74 (2007) 283–287.
[13] C.C. Chen, F.D. Mai, K.T. Chen, C.W. Wu, C.S. Lu, Dyes Pigments 75 (2007) 434–442.
[14] C.H. Chen, C.F. Chang, C.H. Ho, T.L. Tsai, S.M. Liu, Chemosphere 72 (2008) 1712–1720.
[15] S.P. Pablo, A.O. Victor, L.S. Flávio, A.L. Versiane, Biochem. Eng. J. 51 (2010) 194–197.
[16] X.F. Xue, K. Hanna, N.S. Deng, J. Hazard. Mater. 166 (2009) 407–414.
[17] C. Sudalar, G.N. Subbanna, T.R.N. Kutty, J. Phys. Chem. Solids 64 (2003) 2337–2349.
[18] A. Hagfeldt, U. Björksten, S.E. Lindquist, Sol. Energy Mater. Sol. Cells 27 (1992) 293–304.
[19] A.A. Tahir, K.G. Upul Wijayantha, S. Saremi-Yarahmadi, M. Mazhar, V. McKee, Chem. Mater. 21 (2009) 3763–3772.
[20] K.B. Sanjib, M. Nillohit, K.M. Swarup, A. Bibhutosh, M. Anup, Mater. Res. Bull. 45 (2010) 1948–1953.
[21] P. Brezonik, Chemical Kinetics and Process Dynamics in Aquatic Systems, Lewis, Boca Raton, 1993.
[22] Y. Wang, Y.C. Zhao, Y. Ma, H. Liu, Y. Wei, J. Mol. Catal. A: Chem. 325 (2010) 79–83.
[23] C. Gregor, M. Hermanek, D. Jancik, J. Pechousek, J. Filip, J. Hrbac, R. Zboril, Eur. J. Inorg. Chem. (2010) 2343–2351.
[24] R.E. Palma-Goyes, F.L. Guzmán-Duque, G. Peñuela, I. González, J.L. Nava, R.A. Torres-Palma, Chemosphere 81 (2010) 26–32.
[25] Y.M. Ju, J.D. Fang, X.W. Liu, Z.C. Xu, X.W. Ren, C. Sun, S.G. Yang, Q. Ren, Y.C. Ding, K. Yu, L.H. Wang, Z.B. Wei, J. Hazard. Mater. 185 (2011) 1489–1498.
[26] K. Hanna, T. Kone, G. Medjahdi, Catal. Commun. 9 (2008) 955–959.
[27] E.G. Garrido-Ramírez, B.K.G. Theng, M.L. Mora, Appl. Clay Sci. 47 (2010) 182–192.
[28] J.J. Wu, M. Muruganandham, J.S. Yang, S.S. Lin, Catal. Commun. 7 (2006) 901–906.
[29] W.P. Du, Y.M. Xu, Y.S. Wang, Langmuir 24 (2008) 175–181.
[30] M.M. Alnuaimi, M.A. Rauf, S.S. Ashraf, Dyes Pigments 76 (2008) 332–337.
[31] P. Kwan, B.M. Voelker, Environ. Sci. Technol. 37 (2003) 1150–1158.
[32] H. Kong, R.J. Watts, J.H. Choi, Chemosphere 37 (1998) 1473–1482.